Received: 29 October 2018 | Revised: 13 December 2018 | Accepted: 21 December 2018

DOI: 10.1002/aoc.4800

FULL PAPER

WILEY Applied Organometallic Chemistry

Synthesis of multifunctional polymer containing Ni-Pd NPs via thiol-ene reaction for one-pot cascade reactions

Roozbeh Javad Kalbasi | Niloofar Mesgarsaravi | Reza Gharibi

Faculty of Chemistry, Kharazmi University, Tehran, Iran

Correspondence
Roozbeh Javad Kalbasi, Kharazmi University, Tehran, Iran.
Email: rkalbasi@khu.ac.ir; rkalbasi@gmail.com

Recently, acid–base bifunctional catalysts have been considered due to their abilities, such as the simultaneous activation of electrophilic and nucleophilic species and their high importance in organic syntheses. However, the synthesis of acid–base catalysts is problematic due to the neutralization of acidic and basic groups. This work reports a facial approach to solve this problem via the synthesis of a novel bifunctional polymer using inexpensive materials and easy methods. In this way, at the first step, heterogeneous poly (styrene sulfonic acid-*n*-vinylimidazole) containing pentaerythritol tetra-(3-mercaptopropionate) (PETMP) and trimethylolpropane trimethacrylate (TMPTMA) cross-linkers were synthesized in the pores of a mesoporous silica structure using click reaction as a novel bifunctional acid–base catalyst. After that, Ni-Pd nanoparticles supported on poly (styrenesulfonic acid-*n*-vinylimidazole)/KIT-6 as a novel trifunctional heterogeneous acid–base-metal catalyst was prepared. The prepared catalysts were characterized by various techniques like FT-IR, TGA, ICP-AES, DRS-UV, TEM, FE-SEM, EDS-Mapping, and XRD. The synthesized catalysts were efficiently used as bifunctional/trifunctional catalysts for one-pot, deacetalization-Knoevenagel condensation and one-pot, three-step and a sequential reaction containing deacetalization-Knoevenagel condensation-reduction reaction. It is important to note that the synthesized catalyst showing high chemo-selectivity for the reduction of nitro group, alkenyl double bond and ester group in the presence of nitrile. Moreover, it was found that the different nanoparticles including Ni, Pd, and alloyed Ni-Pd showing different chemo-selectivity and catalytic activity in the reaction.

KEYWORDS

Deacetalization-Knoevenagel condensation, Pd-Ni alloy nanoparticles, reduction, thiol-ene click reaction, tri-functional catalyst

1 | INTRODUCTION

One-pot sequential reactions have become an attractive field due to their high importance in organic syntheses.[1–3] The advantages of these reactions include reduce the number of synthesis steps, simple purifications, high performance, high atom economy, reduce wastes, decrease reaction time and recovery capability. In recent years, catalysts including different active groups (multifunctional) on their surface are good candidates for improving multiple reactions in a single pot.[4,5] Among the different multifunctional catalysts that have been presented, most have focused on acid–base bifunctional catalysts with some advantages such as decreasing the number of

 © 2019 John Wiley & Sons, Ltd.

isolation and purification of intermediates. Actually, due to their ability to simultaneously activate electrophilic and nucleophilic species, these kinds of catalysts can be used for one-pot sequential reactions.[6] This ability can increase the overall efficiency of the reactions. Therefore, in the last decades, a large number of bifunctional acid–base homogenous catalysts have been designed to achieve this goal. However, due to the lack of recovery ability, contamination of the product with the catalyst, and neutralization of the acid and base sites, using bifunctional acid–base homogeneous catalysts were limited.[7]

In order to improve the properties of bifunctional homogeneous acid–base catalysts, different research groups have introduced various bifunctional heterogeneous acid–base catalysts and using them in organic reactions.[8–12] Moreover, in addition to these researches, a few works have been reported about the synthesis of heterogeneous trifunctional catalysts containing acidic and basic sites. One of them and the most important one is the catalyst that Biradar et al. prepared and used for one-pot, three-step sequential deacetylation-Henry-hydrogenation reaction.[13] This tri-functional catalyst included sulfonic acid as an acid group, amine as a basic group and Pd as a metal nanoparticle, which was supported on a mesoporous silica. According to these researches, some of the disadvantages of homogeneous catalysts were decreased. However, despite many efforts to the preparation of bifunctional/multifunctional heterogeneous acid–base catalysts for one-pot tandem reactions, many of the synthesized catalysts (some of them are mentioned above) have problems such as the complicated procedure for preparation of the catalyst. Using organosilane compounds are not suitable due to toxicity and high cost and the neutralization of acid–base groups by each other.

In this work, in order to reduce the deficiencies of the previous synthesized heterogeneous acid–base catalysts, we report an effective, facile and novel method to synthesize a trifunctional heterogeneous acid–base-metal catalyst named Ni-Pd@poly (styrenesulfonic acid-*n*-vinylimidazole)/KIT-6 (Ni-Pd@poly (SSA-NVI)/KIT-6). In this regard, at the first step, quite heterogeneous poly (styrenesulfonic acid-*n*-vinylimidazole) containing pentaerythritol tetra (3-mercaptopropionate) (PETMP) as tetra-thiol core and trimethylolpropane trimethacrylate (TMPTMA) species were prepared inside the pores of KIT-6 as a mesoporous silica with a high surface area. Actually, the most common method for the synthesis of poly (styrenesulfonic acid-*n*-vinyl imidazole) is the conventional radical polymerization method.[14] However, the mentioned conventional method has some problems including 1. remaining monomers in the reaction mixture; 2. high sensitivity to radical polymerization relative to oxygen and 3. the possibility of neutralizing acid and base monomers with each other. Recently, "click chemistry" methods offered an excellent opportunity for the preparation and modification of polymeric materials.[15,16] The thiol–ene reaction is one of the most important types of click reactions, which allows simple and efficient synthesis of different polymeric networks. This reaction includes the radical addition of thiol functional groups to electron-rich enes and producing thioether network.[17,18] High efficiency, uniform distribution of monomers in the polymer network, oxygen and moisture insensitivity, inoffensive by-product, and relatively high reaction rates are some of the main advantages of thiol-ene click reaction which are beneficial for the preparation of polymeric network as the heterogeneous acid–base catalyst. It is worth to notice that presence of multifunctional thiol and ene as cross-linkers in the final polymeric network led to the spacing between acid and base groups that could limit the possibility of neutralization of these two groups in the heterogeneous acid–base catalyst. Therefore, in the present study instead of the conventional radical polymerization method utilization of thiol-ene click chemistry for the preparation of cross-linked poly (styrenesulfonic acid-*n*-vinyl imidazole) was considered. Finally, poly (styrenesulfonic acid-*n*-vinylimidazole)/KIT-6 was used as an efficient bifunctional heterogeneous acid–base catalyst for one-pot tandem deacetalization-Knoevenagel condensation reaction. Furthermore, Ni and Pd nanoparticles have been anchored on poly (styrenesulfonic acid-*n*-vinylimidazole)/KIT-6 to prepare a trifunctional heterogeneous acid–base-metal catalyst. The prepared catalyst was effectively used in the one-pot three-step sequential deacetalization-Knoevenagel condensation-reduction reaction with excellent yields and interesting selectivity.

2 | EXPERIMENTAL METHODS

2.1 | Materials and instruments

All materials were purchased from Aldrich and Merck in high purity: *n*-vinylimidazole (NVI), sodium styrene sulfonate (SSNa), Amberjet 1200, azobisisobutyronitrile (AIBN), pentaerythritol tetra-(3-mercaptopropionate) (PETMP), trimethylolpropane trimethacrylate (TMPTMA), tetraethylorthosilicate (TEOS), *n*-butanol, H_2O, hydrochloric acid (HCl), Pluronic P123 triblock copolymer (PEG_{30}-PPG_{70}-PEG_{30}), $NiCl_2$, $PdCl_2$, sodium borohydride ($NaBH_4$) and ethanol were used as received without any further purification.

The catalysts were identified using various techniques. Fourier-transform infrared spectra (FTIR) were used by Perkin Elmer RX1 in KBr pellets or neat liquid technology.

Thermogravimetric (TG) analysis was performed by Perkin Elmer, Pyris1 under a flow of nitrogen by heating from room temperature to 700 °C at a rate of 10 °C min^{-1}. X-ray powder diffractions (XRD) containing small and wide angle, were carried out on a Philips PW1730 X-ray diffractometer by using Ni-filtered Cu-Kα radiation (λ = 0.15418 nm). Field Emission Scanning Electron Microscopy (FESEM), energy dispersive spectroscopy (EDS) and elemental mapping (X-ray mapping) were carried out for defining the morphology, the elemental analysis and the elemental mapping of the catalysts on a TESCAN MIRA instrument. Transmission electron microscope (TEM) images were performed on CM30 300 kV. The pore size distribution and specific surface areas were studied by Barrett–Joyner–Halenda (BJH) and Brunauer–Emmett–Teller (BET) methods by using nitrogen adsorption–desorption measurement at liquid nitrogen temperature (Series SBELSORP MINI). Diffuse reflectance spectra (DRS) UV–Vis spectra were recorded by Scinco 4100 apparatus. The Pd and Ni content in samples were performed by inductively coupled plasma atomic emission spectrometry (ICP-AES) by using Perkin-Elmer optima 4300. All the products were performed by ^{1}HNMR and ^{13}CNMR spectra of Burker Advanced 300 spectrometer at 300.1 and 75 MHz spectrometers, respectively and GC-Mass analysis was carried out by use of Thermoquest–Finnigan Trace GC–Mass instrument equipped with a DB-5 fused silica column (60 m×0.25 mm i.d., film thickness 0.25 mm) and FT-IR instrument.

2.2 | Catalysts preparation

2.2.1 | Preparation of KIT-6

The unique mesoporous silica KIT-6 was synthesized by the reported procedure.[19] It was achieved by using P123 template and TEOS as a structure directing agent and as the silica precursor, respectively. In a typical synthesis, 6 g (1.03 mmol) P123 was dissolved in 270 g (15 mol) deionized water and 11.4 g (0.115 mol) HCl solution (37 wt. %) under stirring. Then, 6 g (0.161 mol) n-butanol was added at once with continuous stirring. Then, after one hour, 12.9 g (0.061 mol) TEOS was added at once to this mixture and was stirred for 24 hr at 35 °C in order to form the meso-structure product. Then, to expand the silica pore diameters, the obtained sol was heated for hydrothermal treatment at 93 °C for another 24 hr, statically. The solid product was filtered and washed by deionized water to remove residue HCl and dried at 100 °C, overnight. Finally, to remove the organic template and obtain highly ordered 3D mesoporous KIT-6, the product was calcined at 550 °C for 6 hr.

2.2.2 | Preparation of poly (styrenesulfonic acid-n-vinylimidazole)/KIT-6 nanocomposite (poly (SSA-NVI)/KIT-6)

To synthesize the polymer in the pores of KIT-6, at first, 0.103 g (0.5 mmol) SSNa was dissolved in 2 ml deionized water. Then, 0.206 g Amberjet 1200 as an ion exchange resin was added and stirred for 1 hr. afterward, the mixture was filtered to obtain styrene sulfonic acid (SSA) monomer. Then, 0.25 g KIT-6 was added to the remained solution and stirred. After one hour, 0.904 g (1 mmol) NVI was added to the mixture and stirred overnight at room temperature. After an interval time, 0.183 g (0.37 mmol) PETMP and 0.025 g (0.064 mmol) TMPTMA and 3 ml ethanol were added to the mixture and it was mixed for another 15 min. Then, radical polymerization was started by adding 0.005 g (0.03 mmol) AIBN at 75 °C for 48 hr via thiol-ene click reaction. Finally, the obtained product was filtered and washed with deionized water and dried overnight at room temperature.

2.2.3 | Preparation of Ni-Pd@poly (styrene sulfonic acid-n-vinylimidazole)/KIT-6 nanocomposite (Ni-Pd@poly (SSA-NVI)/KIT-6)

For the preparation of Ni-Pd@poly (styrene sulfonic acid-*n*-vinylimidazole)/KIT-6 nanocomposite, 0.1 mmol metal chloride containing $NiCl_2$ and $PdCl_2$ mixture with 70:30 molar ratio, respectively, was added to 0.1 g (styrene sulfonic acid-*n*-vinylimidazole)/KIT-6 nanocomposite, together with 3 ml deionized water. For uniform distribution of metals in the nanocomposite, the mixture was located in an ultrasonic bath for 15 min. Then, it was stirred for 4 hrs at 60 °C. After that, a solution of $NaBH_4$ (0.6 mmol $NaBH_4$ with 5 ml deionized water) was added to the mixture drop by drop under N_2 atmosphere and the mixture was stirred for 4 hr at the same constant temperature. Afterward, the final precipitate was filtered and washed sequentially with deionized water to remove excess $NaBH_4$, $NiCl_2$, and $PdCl_2$ and dried at 80 °C for 3 hr. ICP-AES appraised 0.0476 $mmolg^{-1}$ Ni and 0.0213 $mmolg^{-1}$ Pd content of Ni-Pd@poly (SSA-NVI)/KIT-6.

2.3 | General procedure for the one-pot sequential deacetalization–Knoevenagel condensation reaction

In a typical reaction procedure, benzaldehyde dimethylacetal (1 mmol), ethyl cyanoacetate (1 mmol) and poly (SSA-NVI)/KIT-6 (0.03 g) were added to 3 ml

deionized water in a round-bottomed flask. The resulting mixture was stirred at 45 °C for 30 min. Thin layer chromatography (hexane-ethyl acetate with 4:1 ratio) was used to follow the progress of the reaction. After the completion of the reaction, the mixture was cooled down to 10 °C, filtered and the remaining solid was washed by hot ethanol (10 ml). Afterward, the precipitate appeared in the solution. After crystallization, the final product was isolated to achieve a pure product. Resulting product obtained in 93% yield and was identified by ^{1}H-NMR, ^{13}C-NMR, and FT-IR spectroscopies.

2.3.1 | Ethyl (E)-2-cyano-3-(2-nitrophenyl) acrylate

FT-IR (KBr, cm^{-1})

3071–3032 (=CH, Ar, str.), 2987 (CH, str.), 2226 (CN), 1718 (C=O), 1606–1472 (C=C alkene, C=C aromatic), 1529–1355 (N=O); **^{1}H NMR (300 MHz, $CDCl_3$,Hz) δ ppm:** 8.70 (=CH, s, 1H), 8.39–8.44 (ArH, m, 2H), 8.31 (ArH, s, 1H), 7.74 (ArH, t, 1H, J = 8.1), 4.43 (CH_2-O, q, 2H, J = 7.2), 1.42(CH_3, t, 3H, J = 7.2);); **^{13}CNMR (75 MHz, $CDCl_3$) δ ppm:** 167.4 (C=O), 151.8, 145.4, 135.1, 132.8, 130.5, 127.0, 125.8, 114.5 (CN), 106.6 (C-CN), 63.1 (C-O), 14.1.

2.3.2 | Ethyl (E) - 2-cyano-3- (p-tolyl) acrylate

FT-IR (KBr, cm^{-1})

3028 (=CH, Ar, str.), 2985 (CH, str.), 2217 (CN), 1722(C=O), 1597–1462 (C=C alkene, C=C aromatic); **^{1}H NMR (300 MHz, $CDCl_3$, Hz) δ ppm**: 8.22 (=CH, s, 1H), 7.92–7.89 (ArH, d, 2H, J = 8.7), 7.32–7.26 (ArH, d, 2H, J = 8.7), 4.42–4.35 (CH_2-O, q, 2H, J = 7.2), 2.44 (CH_3-Ar, s, 3H), 1.42(CH_3, t, 3H, J = 7.2); **^{13}CNMR (75 MHz, $CDCl_3$) δ ppm**: 162.8 (C=O), 155.0 (C-Ar), 144.6, 131.2, 130.0, 128.8, 115.8(CN), 62.6(C-O), 21.9(CH_3-Ar), 14.1.

2.3.3 | Ethyl (E)-2-cyano-3-(thiophen-2-yl) acrylate

FT-IR (KBr, cm^{-1})

3086, 3027 (=CH, Ar, str.), 2975 (CH, str.), 2218 (CN), 1715(C=O), 1597–1464 (Ar, str.); **^{1}H NMR (300 MHz, $CDCl_3$,Hz) δ ppm:** 8.35 (=CH, s, 1H), 7.84 (ThiO-H, d, 1H, J = 3.9), 7.79 (ThiO-H, d, 1H, J = 5.1), 7.23 (ThiO-H, dd, 1H, *3 J* = 5.1, *4 J* = 3.9), 4.37 (CH_2-O,, q, 2H, J = 7.2), 1.39(CH_3, t, 3H, J = 7.2); **^{13}CNMR (75 MHz, $CDCl_3$) δ ppm:** 162.6 (C=O), 146.6, 137.1, 136.0, 135.1, 128.6, 115.7(CN), 99.3(C-CN), 62.5 (C-O), 14.1.

2.3.4 | Ethyl (E)-3-(4-chlorophenyl)-2-cyanoacrylate

FT-IR (KBr, cm^{-1})

3036 (=CH, Ar, str.), 2990 (CH, str.), 2223 (CN), 1723(C=O), 1612–1491 (Ar, str.), 832(C-Cl); **^{1}H NMR (300 MHz, $CDCl_3$,Hz) δ ppm**: 8.20 (=CH, s, 1H), 7.95 (ArH, d, 2H, J = 8.7), 7.49 (ArH, d, 2H, J = 8.7), 4.40 (CH_2-O, q, 2H, J = 7.2), 1.42(CH_3, t, 3H, J = 7.2); **^{13}CNMR (75 MHz, $CDCl_3$) δ ppm**: 162.2 (C=O), 153.4 (C-Ar), 132.2(C-Cl), 131.36, 129.8, 129.6, 115.2(CN), 103.5(C-CN), 62.8 (C-O), 14.1.

2.3.5 | Ethyl (E)-2-cyano-3-(2, 6-dichlorophenyl) acrylate

FT-IR (KBr, cm^{-1})

3075, 3036 (=CH, Ar, str.), 2981 (CH, str.), 2236 (CN), 1722(C=O), 1555–1476 (Ar, str.), 797(C-Cl); **^{1}H NMR (300 MHz, $CDCl_3$,Hz) δ ppm:** 8.29 (=CH, s, 1H), 7.31–7.44 (ArH, m, 3H), 4.42 (CH_2-O, q, 2H, J = 7.2), 1.43(CH_3, t, 3H, J = 7.2); **^{13}CNMR (75 MHz, $CDCl_3$) δ ppm:** 160.6 (C=O), 151.1 (C-Ar), 134.1, 131.6, 130.3, 128.5, 113.9 (CN), 113.3(C-CN), 63.1(C-O), 14.0.

2.3.6 | Ethyl (E)-2-cyano-3-(4-methoxyphenyl) acrylate

FT-IR (KBr, cm^{-1})

3028 (=CH, Ar, str.), 2991 (CH, str.), 2215 (CN), 1718 (C=O), 1585–1475 (C=C alkene, C=C aromatic); **^{1}H NMR (300 MHz, $CDCl_3$,Hz) δ ppm:** 8.17 (=CH, s, 1H), 8.1 (ArH, d, 2H, J = 9), 7.00 (ArH, d, 2H, J = 9), 4.37 (CH_2-O, q, 2H, J = 7.2), 3.90(CH_3-O,S, 3H) 1.39 (CH_3, t, 3H, J = 7.2); **^{13}CNMR (75 MHz, $CDCl_3$) δ ppm:** 163.7 (C=O), 163.1, 154.3 (C-Ar), 133.6, 124.3, 116.2(CN), 114.7, 99.3 (C-CN), 62.4 (C-O), 55.5 (CH_3O), 14.1.

2.4 | General procedure for the one-pot sequential deacetalization-Knoevenagel condensation-reduction reaction

The reaction mixture composed of benzaldehyde dimethylacetal (1 mmol), ethyl cyanoacetate (1 mmol), Ni-Pd@poly (SSA-NVI)/KIT-6 (0.03 g) and deionized water (3 ml) was added in a glass reactor. The resulting mixture was stirred at 45 °C for 30 min. Thin layer chromatography (hexane-ethyl acetate with 4:1 ratio) was used to follow the progress of the reaction. After the completion of the deacetalization-Knoevenagel condensation reaction, 1 mmol $NaBH_4$ was added to the reaction mixture and the resulting mixture was stirred at 45 °C for 20 min. Thin layer chromatography (hexane-ethyl acetate

with 3:2 ratio) was used to follow the progress of the reaction. After the completion of the reaction, the mixture was cooled to room temperature. Then, the product of reduction (organic phase) was extracted with chloroform (2 × 10 ml) and the organic phase was dried over anhydrous Na_2SO_4. The suspension was filtered and the solvent was evaporated under vacuum to give the desired product. To achieve pure product, TLC on 60 F_25_4 silica gel plates was used. The final product was characterized by FT-IR, ^{1}HNMR, ^{13}CNMR and GC-Mass techniques. This product was obtained in 94% yield.

2.4.1 | 2-(3-aminobenzyl)-3-hydroxypropanenitrile

FT-IR (KBr, cm^{-1})

3358(NH_2), 3043 (=CH, Ar, str.), 2993 (CH, str.), 2242 (CN), 1606–1463 (Ar, str.); **^{1}H NMR (300 MHz, $CDCl_3$, Hz) δ ppm:** 7.08–7.17 (ArH, m, 1H), 6.57–6.75 (ArH, m, 3H), 3.67–3.76 (CH_2, m, 2H), 2.85–4.24 (OH, NH_2, br, 3H), 2.85–2.95 (CH_2, CH, m, 3H); **^{13}CNMR (75 MHz, $CDCl_3$) δ ppm:**146.6 (C), 137.5 (C), 129.7 (C), 119.1 (CN), 117.1, 115.5, 114.0 (CH), 61,7 (CH_2-OH), 36.5 (CH_2), 34.4 (CH-CN); **LRMS m/z (Abund %)** 176 [$M^{+\cdot}$] (31.9), 128 (6.3), 107 [106-$H^{+\cdot}$] (100), 106 [NH_2-Ph-$CH_2^{+\cdot}$] (76), 93 (5.1), 77 (15.4).

2.4.2 | 3-hydroxy-2-(4-methoxybenzyl) propanenitrile

FT-IR (KBr, cm^{-1})

3459(OH), 3032 (=CH, Ar, str.), 2927 (CH, str.), 2242 (CN), 1513–1612 (Ar, str.), **^{1}H NMR (300 MHz, $CDCl_3$, Hz) δ ppm:** 7.16 (ArH, d, 2H, J = 8 Hz), 6.86 (ArH, d, 2H, J = 8 Hz), 3.78 (OMe, s, 3H), 3.67–3.74 (CH_2-O, m, 2H), 2.9 (CH-CN, CH_2-Ar, m, 3H), 2.61(OH, s, 1H).

2.4.3 | 2-benzyl-3-hydroxypropanenitrile

FT-IR (KBr, cm^{-1})

3430(OH), 3030 (=CH, Ar, str.), 2934 (CH, str.), 2245 (CN), 1497–1603 (Ar, str.); **^{1}H NMR (300 MHz, $CDCl_3$,Hz) δ ppm:** 7.25–7.37 (ArH, m, 5H), 3.73–3.83 (CH_2-OH, m, 2H), 2.9–3.1 (CH-CN, CH_2-Ar, m, 3H), 2.16 (OH, s, 1H); **^{13}CNMR (75 MHz, $CDCl_3$) δ ppm:** 136.3, 128.9, 128.8, 127.3, 120.3 (CN), 61.7 (C-O), 36.7 (C-Ph), 34.4 (C-CN).

2.4.4 | 2-(4-fluorobenzyl)-3-hydroxypropanenitrile

FT-IR (KBr, cm^{-1})

3441(OH), 3042 (=CH, Ar, str.), 2927 (CH, str.), 2244 (CN), 1511–1601 (Ar, str.); **^{1}H NMR (300 MHz, $CDCl_3$, Hz) δ ppm:** 7.19–7.26 (ArH, m, 2H), 6.99–7.06 (ArH, m, 2H), 3.70–3.81 (CH_2-O, m, 2H), 2.87–2.97 (CH-CN, CH_2-Ar, m, 3H), 2.36(OH, s, 1H); **^{13}CNMR (75 MHz, $CDCl_3$) δ ppm:** 163.69, 160.4(C-F), 132.0, 132.0, 130.6, 130.5, 120.2 (CN), 115.8, 115.54, 61.6 (C-O), 36.8 (C-Ar), 33.6 (C-CN).

3 | RESULTS AND DISCUSSION

As explained in the experimental section, poly (SSA-NVI)/KIT-6 was synthesized via the in situ polymerization of styrene sulfonic acid and n-vinyl imidazole in the presence of PETMP as tetra-thiol core and TMPTMA through a click type reaction in the pores of KIT-6 mesoporous silica material. Also, Ni-Pd@poly (SSA-NVI)/KIT-6 was fabricated through the anchoring of Ni-Pd alloy nanoparticles on poly (SSA-NVI)/KIT-6. Figure **1** shows a schematic description of the steps for the preparation of Ni-Pd@poly (SSA-NVI)/KIT-6.

3.1 | Characterization of the catalysts

The FT-IR spectra of PETMP (tetra thiol core) and TMPTMA species and cross-linked poly (SSA-NVI) are presented in Figure 2. For PETMP, the peak at 2959 cm^{-1} is assigned to the aliphatic C-H stretching vibration and the peaks at 2567 cm^{-1} and 1735 cm^{-1} are related to the S-H and C=O stretching vibration of PETMP.[19] For TMPTMA, the peaks at 3104 cm^{-1}, 2961 cm^{-1}, 1735 cm^{-1}, and 1639 cm^{-1} are related to alkene C-H stretching vibration, aliphatic C-H stretching vibration, C=O stretching vibration and olefinic C=C stretching vibration, respectively.[20]

For the cross-linked poly (SSA-NVI), the shown peak at 3434 cm^{-1}, 1356 cm^{-1}, and 1189 cm^{-1} are attributed to the hydroxyl group of SO_3H and asymmetric as well as symmetric stretching vibration of S=O group, respectively, which are related to the poly (styrenesulfonic acid).[21] Also, the peak at 1468 cm^{-1} is related to the C=N bond of poly *n*-vinylimidazole. Moreover, the peaks at 3116 cm^{-1} and 2969 cm^{-1} are indicated the stretching vibration of aromatic and aliphatic C-H, respectively, which are related to cross-linked poly (SSA-NVI).[22] Actually, the absence of the peaks at 2567 cm^{-1} (S-H) and 1650 cm^{-1} (C=C) and the existence of the peak at 1735 cm^{-1} (C=O) in FT-IR spectrum of cross-linked poly (SSA-NVI) indicate that PETMP and TMPTMA are successfully entered into the poly (SSA-NVI) structure. Finally, these evidence show the successful formation of cross-linked poly (SSA-NVI) through thiol-ene click reaction.

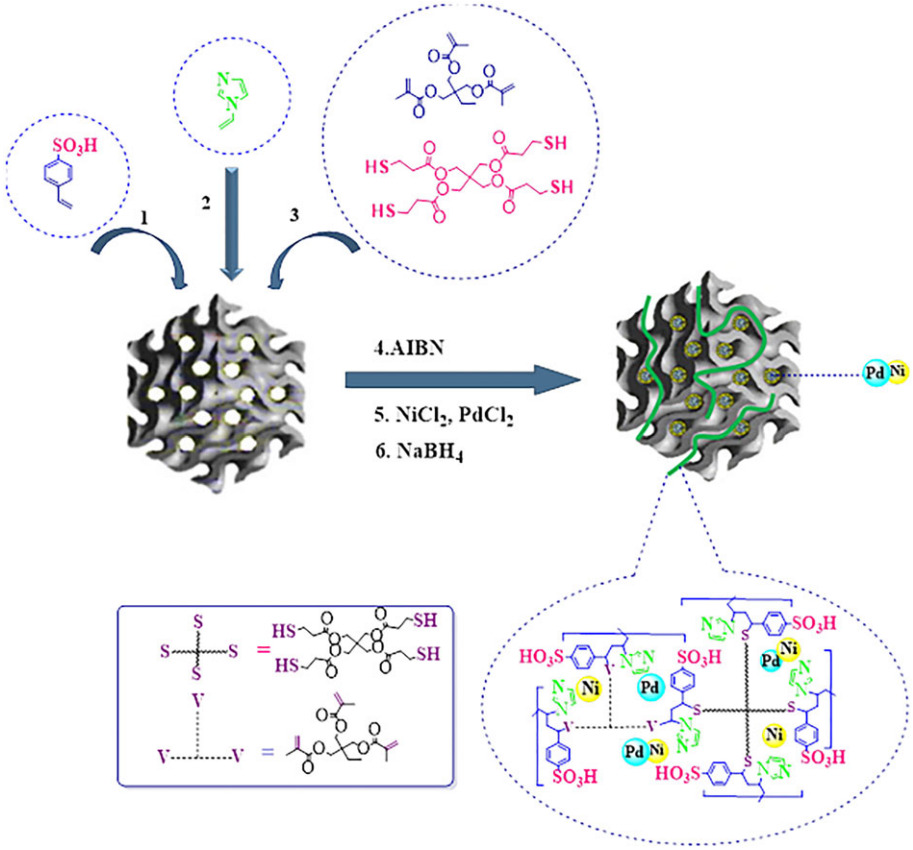

FIGURE 1 Synthesis of Ni-Pd@poly (SSA-NVI)/KIT-6

Furthermore, FT-IR spectra of pure KIT-6 and poly (SSA-NVI)/KIT-6 nanocomposite are shown in Figure 2. The FT-IR spectrum of pure KIT-6 shows two bands at 3459 cm^{-1} and 1635 cm^{-1} which are related to the stretching and bending vibration of the adsorbed water molecules on the surface and OH of internal silanol groups of KIT-6. Also, the very strong and broad peak at 1082 cm^{-1} and the peak at 803 cm^{-1} are attributed to the asymmetric and symmetric stretching vibrations, respectively and the peak at 461 cm^{-1} is assigned to the bending vibration of Si-O-Si bonds of KIT-6.[23]

As shown in poly (SSA-NVI)/KIT-6 nanocomposite spectrum, all the peaks of the KIT-6 are displayed which indicate the presence of KIT-6 in the nanocomposite structure. Also, all of the poly (SSA-NVI) peaks which described in Figure 2 are observed in the nanocomposite spectrum, that proves the successful synthesis of the desired nanocomposite (poly (SSA-NVI)/KIT-6).

The low-angle XRD patterns of poly (SSA-NVI)/KIT-6 and Ni-Pd@poly (SSA-NVI)/KIT-6 are displayed in Figure 3a. For both of poly (SSA-NVI)/KIT-6 and Ni-Pd@poly (SSA-NVI)/KIT-6, the small peaks at 1.44°, 2°, and 2.26 ° are attributed to (211),) 220) and (320) diffraction planes of ordered three-dimensional cubic Ia3d symmetry of KIT-6, which exists in the structure of these composites.[24] It is important to note that the above-mentioned peaks in these composites are broader than the pure KIT-6, which is due to the sectional blocking of mesoporous KIT-6 by poly (SSA-NVI) and also the distribution of Pd and Ni nanoparticles in their structures.

Figure 3b shows the wide-angle XRD patterns of the Ni@poly (SSA-NVI)/KIT-6, Pd@poly (SSA-NVI)-KIT-6 and Ni-Pd@poly (SSA-NVI)/KIT-6 nanocomposites. For all samples, a broad peak at $2\theta = 20–30$ is related to the amorphous silica structure of mesoporous KIT-6. The XRD of Pd@poly (SSA-NVI)/KIT-6 exhibits the peaks at 39.8°, 46.85°, and 68.2°, which indicate the (111), (200) and (220) lattice planes of fcc crystalline structure of metallic Pd.[25] Also, any clear peaks were observed for Ni@poly (SSA-NVI)/KIT-6, which could be due to the amorphous nature and small size of Ni nanoparticles.[26] Furthermore, the XRD of Ni-Pd@poly (SSA-NVI)/KIT-6 shows (111) diffraction peak of Pd at 40.05°. This peak was appeared in low intensity at higher 2θ compared with Pd@poly (SSA-NVI)/KIT-6, which indicates the formation of alloy between Ni and Pd in the Ni-Pd@poly (SSA-NVI)/KIT-6.[27]

Figure 4 displays the N_2 adsorption–desorption isotherms and BJH pore size distributions of poly (SSA-NVI)/KIT-6 and Ni-Pd@poly (SSA-NVI)/KIT-6. The N_2 adsorption–desorption isotherm of poly (SSA-NVI)/KIT-6 shows type IV isotherm with hysteresis loop in

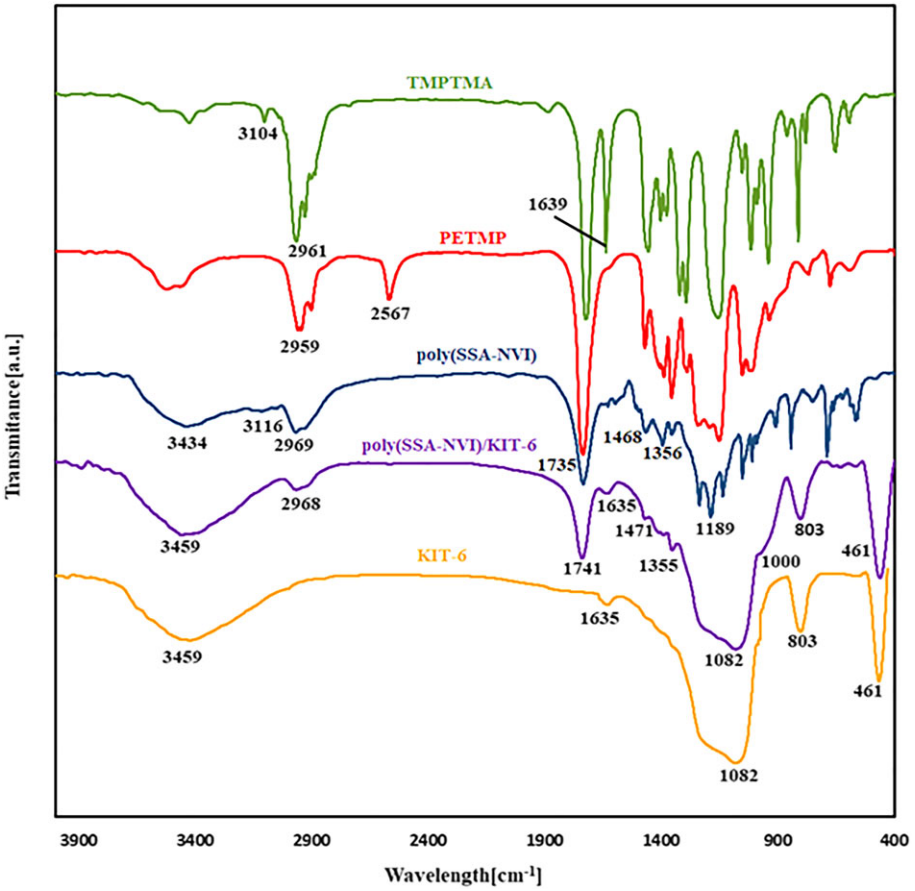

FIGURE 2 FT-IR spectra of TMPTMA, PETMP, poly (SSA-NVI), KIT-6 and poly (SSA-NVI)/KIT-6

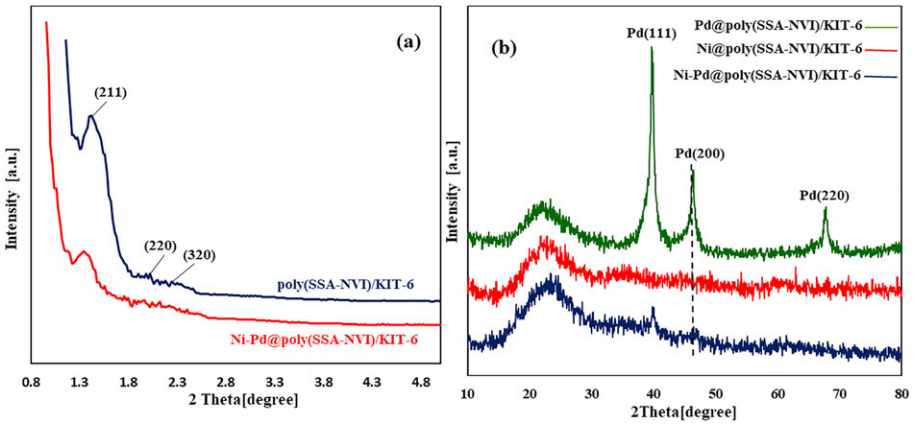

FIGURE 3 (a) Low-angle XRD patterns of Poly (SSA-NVI)/KIT-6 and Ni-Pd@Poly (SSA-NVI)/KIT-6; (b) Wide-angle XRD patterns of Pd@poly (SSA-NVI)/KIT-6, Ni@poly (SSA-NVI)/KIT-6 and Ni-Pd@poly (SSA-NVI)/KIT-6

the p/p_0 at 0.4–1.0, which indicates the mesoporous structure of this sample.[28] Also, the N_2 adsorption–desorption isotherm of Ni-Pd@poly (SSA-NVI)/KIT-6 displays type IV isotherm with hysteresis loop in the p/p_0 at 0.4–1.0 like poly (SSA-NVI)/KIT-6. This result confirms that the mesoporous structure of poly (SSA-NVI)/KIT-6 is preserved in Ni-Pd@poly (SSA-NVI)/KIT-6 after the incorporation of metal nanoparticles. Furthermore, some physical properties such as surface area, pore volume, and pore diameter of these samples are listed in Table 1. The surface area and pore volume of poly (SSA-NVI)/KIT-6 are 258 $m^2\ g^{-1}$ and 0.56 $cm^3\ g^{-1}$, respectively. However, both of these parameters were decreased to 174 $m^2\ g^{-1}$ and 0.45 $cm^3\ g^{-1}$ in Ni-Pd@poly (SSA-NVI)/KIT-6, that these results suggest the incorporation of Ni and Pd nanoparticles in the pores of poly

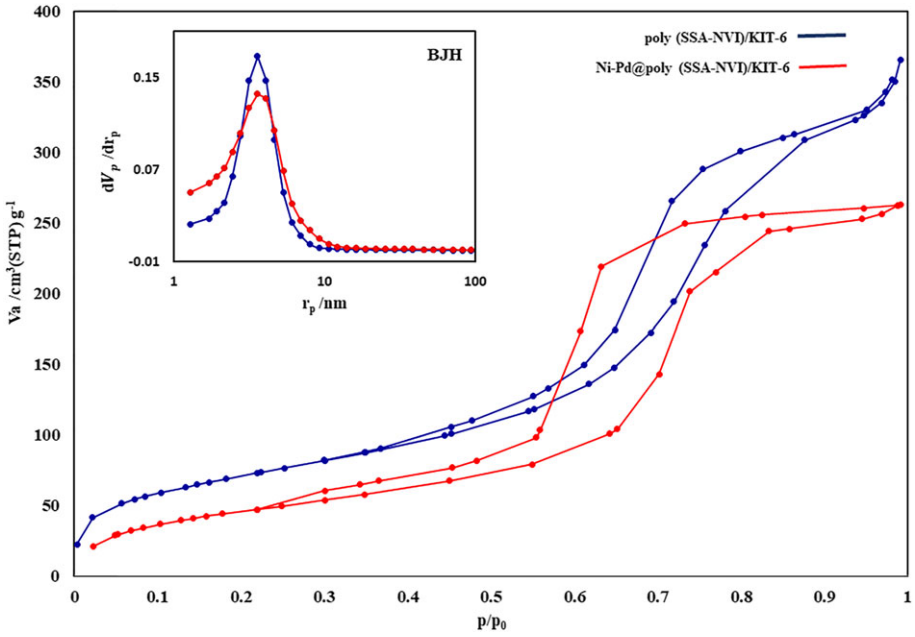

FIGURE 4 N_2 adsorption–desorption isotherms of poly (SSA-NVI)/KIT-6 and Ni-Pd@poly (SSA-NVI)/KIT-6. Inside: BJH pore sizes of poly (SSA-NVI)/KIT-6 and Ni-Pd@poly (SSA-NVI)/KIT-6

TABLE 1 Physicochemical parameters of poly (SSA-NVI)/KIT-6 and Ni-Pd@poly (SSA-NVI)/KIT-6 obtained from N_2 adsorption–desorption analysis

Sample	Smesopore[a] [m2 g^{-1}]	Vmesopore[a] [cm3 g^{-1}]	Dmesopore[b] [nm]	Smicropore[c] [m2 g^{-1}]	Vmicropore[c] [cm3 g^{-1}]	Dmicropore[c] [nm]
poly (SSA-NVI)/KIT-6	258	0.56	7	350	0.1	1.8
Ni-Pd@ poly (SSA-NVI)/KIT-6	174	0.45	8	266	0.08	1.8

[a]Calculated by BET method.

[b]Mean pore diameter determined using BJH method.

[c]Calculated by MP-Plot method.

(SSA-NVI)/KIT-6.[29–31] From Table 1, the pore diameter of poly (SSA-NVI)/KIT-6 is 7 nm. However, after the incorporation of metal nanoparticles, it is enhanced to 8 nm in Ni-Pd@poly (SSA-NVI)/KIT-6, which it can be related to the physical pressure of these nanoparticles from inside to the wall of the pores.[32,33] In addition, the MP-plot and t-plot confirm the existence of micropores beside of the mesopores for both poly (SSA-NVI)/KIT-6 and Ni-Pd@poly (SSA-NVI)/KIT-6 (Table 1), and also the diameters of micropores are equal for these samples, which shows that the Ni-Pd nanoparticles are just placed into the mesopores. Finally, based on the above-mentioned results, it was found that poly (SSA-NVI)/KIT-6 and Ni-Pd@poly (SSA-NVI)/KIT-6 have the meso-micro hierarchical porous structures.

The FE-SEM images of poly (SSA-NVI)/KIT-6 and Ni-Pd@poly (SSA-NVI)/KIT-6 are displayed in Figure **5**. The FE-SEM image of poly (SSA-NVI)/KIT-6 shows the rock-like structure of KIT-6[34] (Figure **5**a). The images of Ni-Pd@poly (SSA-NVI)/KIT-6 display the same structure of support, but the surface seems a little rough, which it could be related to the incorporation of Ni and Pd nanoparticles (Figure **5**b and c).

Furthermore, the EDS analysis and FE-SEM-elemental mapping of poly (SSA-NVI)/KIT-6 show the presence of N, S, C, Si and O on the selected area of the surface, which confirm the successful formation of poly (SSA-NVI) on the surface of KIT-6 (Figure **6**a and b).

The EDS analysis and FE-SEM-elemental mapping of Ni-Pd@poly (SSA-NVI)/KIT-6 show the presence of Ni and Pd in addition to N, S, C, Si and O (Figure 7a and b). Also based on the images of elemental mapping analysis, it was found that Ni and Pd have a uniform distribution on the selected area of the surface. According to the EDS results, the atomic molar ratio of Ni:Pd was calculated 1.31, while it was determined 2.23 based on the ICP-AES. This difference indicates that the main amount of Pd nanoparticles are on the outer surface of Ni-

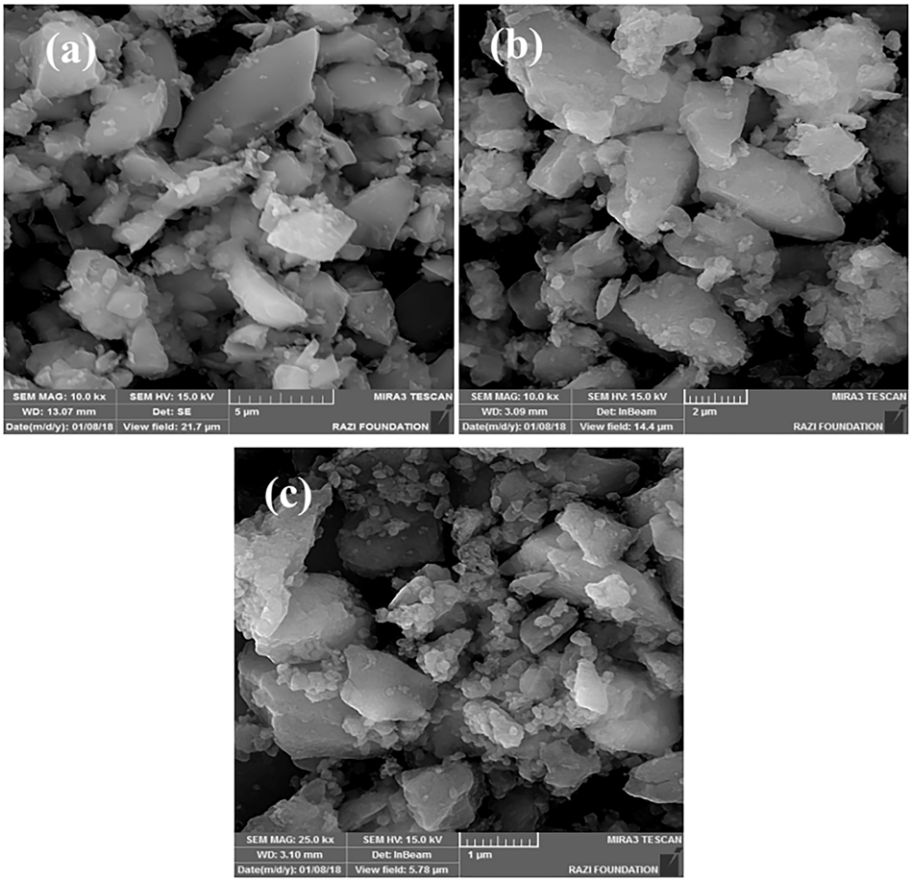

FIGURE 5 (a) FESEM image of poly (SSA-NVI)/KIT-6 and (b, c) FESEM images of Ni-Pd@poly (SSA-NVI)/KIT-6

Pd@poly (SSA-NVI)/KIT-6. Also, it should be noted that EDS is a qualitative analysis and ICP-AES is a technique to determine the exact amount of nanoparticles.

TEM images of Ni-Pd@poly (SSA-NVI)/KIT-6 are shown in Figure 8. These images show a highly ordered cubic *Ia3d* pore channels, which exist in the structure of Ni-Pd@poly (SSA-NVI)/KIT-6 and are belonged to the KIT-6 structure. The dark parts in the images are assigned to Pd and Ni nanoparticles, which distributed on the surface and into the channels of the nanocomposite.[35,36] It is important to note that the regular and uniform structure of KIT-6 remained without any changing after polymerization and incorporation of metal nanoparticles. This result is confirmed by the SEM-EDS, XRD, and N_2 adsorption–desorption.

Figure 9 shows DRS UV–Vis spectra of poly (SSA-NVI)/KIT-6, Ni^{+2}-Pd^{+2}@poly (SSA-NVI)/KIT-6 and Ni-Pd@poly (SSA-NVI)/KIT-6 samples. For Ni^{+2}-Pd^{+2}@poly (SSA-NVI)/KIT-6, the peaks at 265, 314 and 370 nm are assigned to Pd^{+2} and the peaks at 361 and 580 nm are related to Ni^{2+}.[37,38] For Ni-Pd@poly (SSA-NVI)/KIT-6, the intensity of the above-mentioned peaks is decreased, and also the peak of Ni^{2+} at 580 nm disappeared, which indicate to the reduction of Ni^{+2} and Pd^{+2} to Ni and Pd nanoparticles.

The thermal stability of samples was determined by thermogravimetric analysis. The thermal degradation study of samples was done in an N_2 environment at a heating rate of 10 °C/min. The corresponding TGA and DTGA thermograms of poly (SSA-NVI)/KIT-6 and Ni-Pd@poly (SSA-NVI)/KIT-6 are collected in Figure 10a and b, respectively. For both samples, the observed weight loss below 100 °C is related to the loss of physically adsorbed water. Both samples showed a two-step degradation profile. The first transition started at about 290 °C was related to the thermal dissociation of steric groups of PETMP and TMPTMA as cross-linkers and sulfonic acid groups of polymer networks. The second main thermal degradation event at a 462 °C (19% *w*/w) for poly (SSA-NVI)/KIT-6 and 365 °C (12% w/w) for Ni-Pd@poly (SSA-NVI)/KIT-6 was attributed to the scission of aliphatic and aromatic segments of polymeric networks.

It is important to note that the second weight loss of Ni-Pd@poly (SSA-NVI)/KIT-6 was happened at a lower temperature compared to poly (SSA-NVI)/KIT-6, which could be related to the catalytic effect and thermal conductivity of Ni-Pd nanoparticles. Based on these results, it was understood that both of poly (SSA-NVI)/KIT-6 and Ni-Pd/poly (SSA-NVI)/KIT-6 are thermally stable below 290 °C.

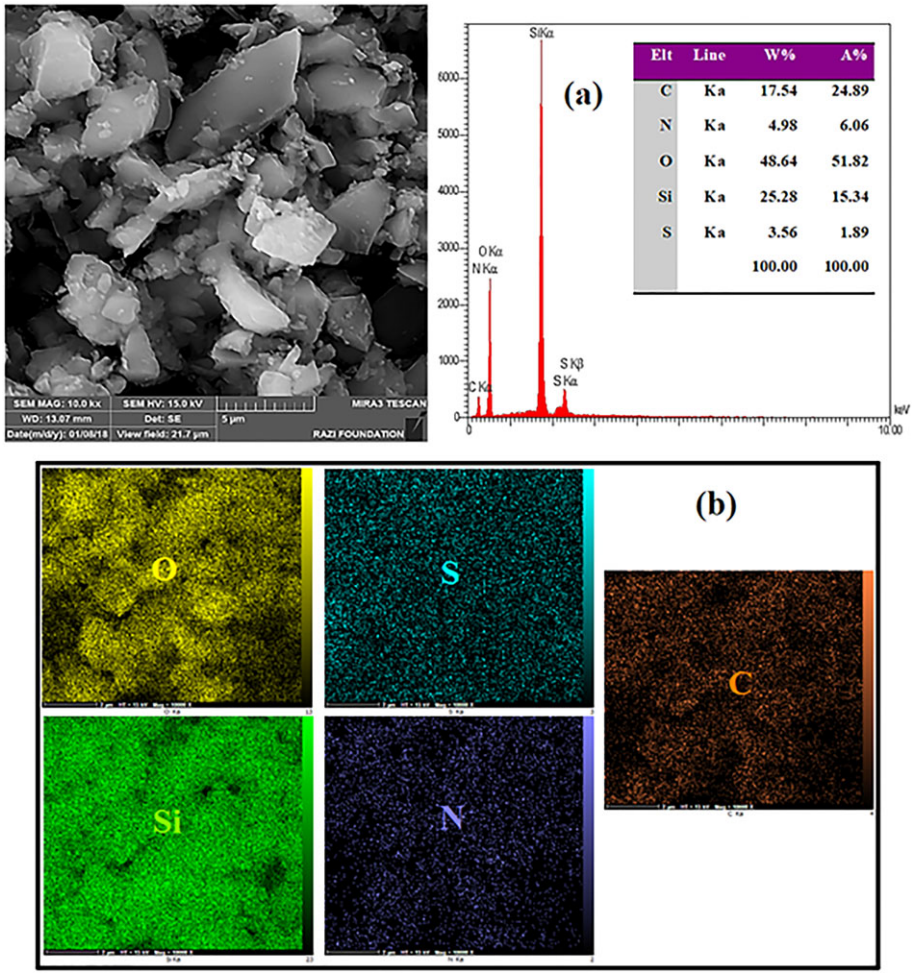

FIGURE 6 (a) EDS analysis and (b) FESEM-elemental-mapping images of poly (SSA-NVI)/KIT-6

3.2 | Catalytic activity

In this study, poly (SSA-NVI)/KIT-6 and Ni-Pd@poly (SSA-NVI)/KIT-6 nanocomposites were synthesized as novel polymeric heterogeneous catalysts, and they were characterized by various techniques.

Poly (SSA-NVI)/KIT-6 was used as an acid–base bifunctional catalyst to perform a sequential one-pot deacetalization–Knoevenagel condensation reaction at 45 °C in the presence of water as solvent, which the acidic groups catalyze the first step (hydrolysis of benzaldehyde dimethyl acetal) and the basic groups catalyze the second step (Knoevenagel condensation) (Scheme 1).

Due to the presence of acidic and basic groups in the polymer network, the amount of polymer which was used for the preparation of the catalyst plays a significant role. Regarding this point, the desired reactions were studied in the presence of different monomeric ratios used for the preparation of the catalyst, while the amount of KIT-6 was fixed (0.25 g) (Table 2, entries 1,2,5). According to the results presented in Table 2, it can be found that the catalyst prepared by 2:1 monomer molar ratio of styrenesulfonic acid to *n*-vinyl imidazole (entry 2), has the best yield at the lowest reaction time. Also, in order to investigate the effect of the amount of KIT-6 silica support on the reaction process, different values of KIT-6 (0.25, 0.5 and 1 g) were used to prepare the nanocomposite while the monomeric molar ratio was fixed at 2:1 (Table 2, entries 2–4). Actually, the role of KIT-6 is acting as a mesoporous support to well distributing of polymer chains and increasing the surface area of the catalyst as well as heterogeneity. According to the results presented in Table 2, with increasing the amount of KIT-6, the yield of the reaction decreases. Actually, in the one hand, increasing the amount of KIT-6 more than 0.25 g cause to an excessive increase in the surface area of the catalyst. On the other hand, it leads to reduce the amount of polymer and subsequently, reduce the amount of active acidic and basic groups at the surface of the nanocomposite. Therefore, it ultimately reduces the catalytic activity. Thus, the catalyst containing the amount of 0.25 g of KIT-6 was selected as an optimum nanocomposite.

Moreover, in order to find a good reason for the effect of monomer molar ratio on the catalytic activity of poly

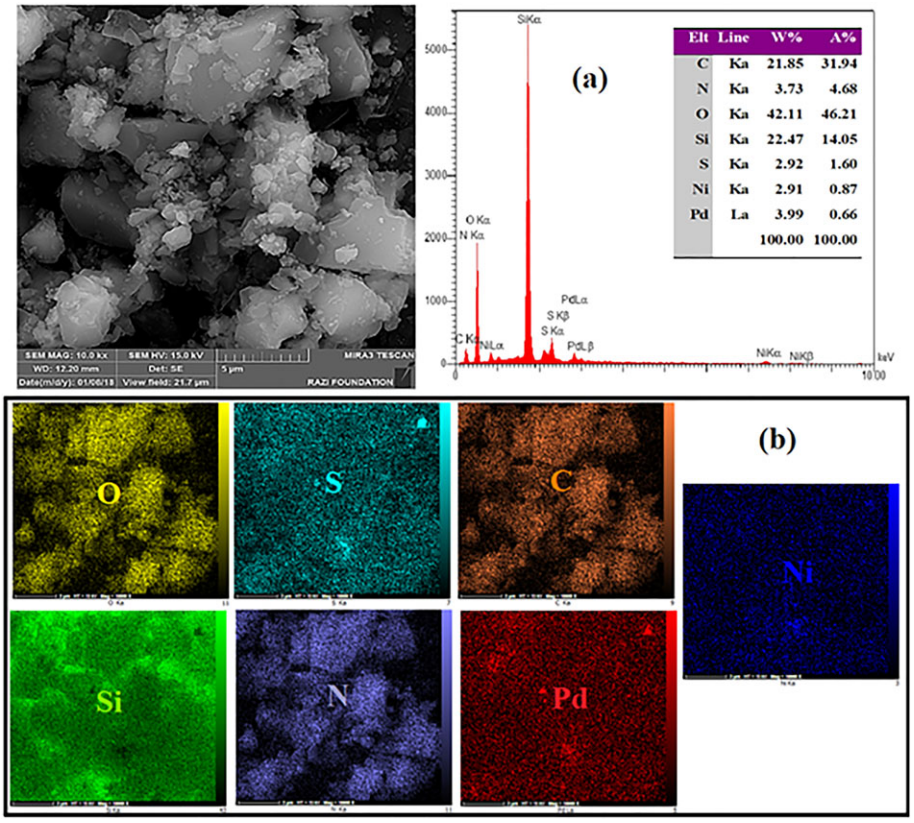

FIGURE 7 (a) EDS analysis and (b) FESEM-elemental-mapping images of Ni-Pd@ Poly (SSA-NVI)/KIT-6

(SSA-NVI)/KIT-6, the amount of acidic and basic sites of the catalysts prepared by various amount of monomer molar ratio were measured by a back titration method which, the results are shown in Table 3 and 4. To measure, poly (SSA-NVI)/KIT-6 composite (0.1 g) was added to a test tube, and 15 ml H_2O with HCl 0.1 M (or 0.1 M NaOH) solution were added. The mixture was stirred for an hour at ambient temperature, then the mixture was filtered and rinsed with 5 ml deionized water. The resulting filtrate was titrated with 0.1 M NaOH (or 0.1 M HCl) solution by using phenolphthalein as an indicator. According to the Table 3, it is observed that the catalyst with 2:1 molar ratio of SSA:NVI (styrenesulfonic acid to n-vinyl imidazole) give a loading of 0.82 mmol g^{-1} (theoretical value, 0.88 mmol g^{-1}) of sulfonic acid groups (Table 3, entry 2) and 0.132 mmol g^{-1} (theoretical value, 0.177 mmol g^{-1}) of amine groups (Table 4, entry 2). Therefore, the percentage of available (free) amine is 74% and the free acid percentage is 93%. By comparing this catalyst with other catalysts prepared with different molar ratios, it is found that the catalyst prepared with 2:1 molar ratio of SSA:NVI has the highest amount of free acid and base sites, together (Table 3 and Table 4). This represents the better catalytic feature of the catalyst prepared by 2:1 monomer molar ratio, so this ratio can be chosen as an optimum amount.

Furthermore, to investigate the role of cross-linkers, a similar catalyst was prepared without using cross-linkers and it was compared with the catalyst prepared with cross-linkers. First of all, it was revealed that the polymer prepared without cross-linkers has the potential for solubility in ethanol and water (the catalyst was not heterogeneous), but with the using of cross-linkers in the polymer network, the polymer doesn't dissolve in as mentioned solvents and the catalyst was completely heterogeneous. Secondly, the results showed that the presence of cross-linkers have increased the yield of polymerization, distinctly (Table S1). Finally, the catalytic activity of these catalysts was compared for one-pot deacetalization–Knoevenagel condensation reaction and the results showed the superior activity of the catalyst which was prepared using cross-linkers (Table S2).

These results show that using the thiol-ene method and PETMP and TMPTMA as cross-linkers which can act as a spacer between acid and base group, most of the acidic and basic sites of the catalyst are free and neutralization of these two groups is minimized.

Another factor that plays an important role in the reaction process is the amount of consumable catalyst that contains acid and base active sites.

According to Table 5, when the catalyst value is less than 0.03 g, the yield of the reaction is not acceptable (entry 1). Also, when the amount of catalyst increases to

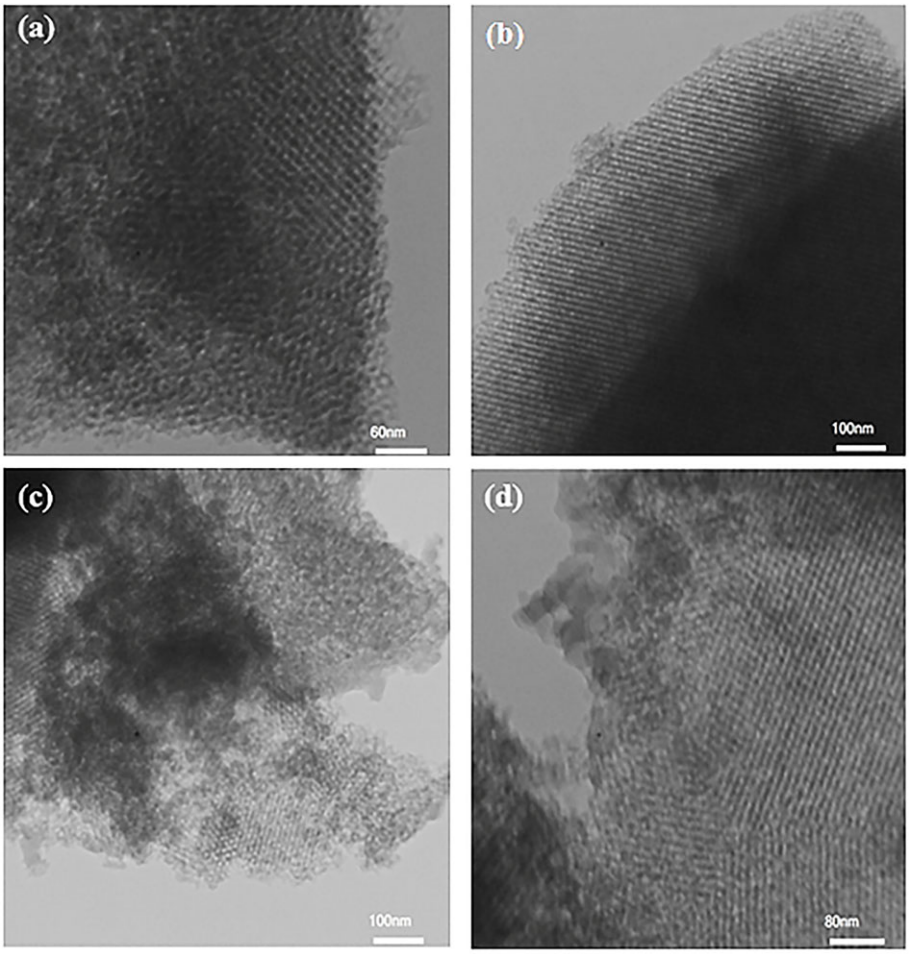

FIGURE 8 TEM images of Ni-Pd@poly (SSA-NVI)/KIT-6

more than 0.03 g, there is no significant effect on the yield of the reaction. Therefore, considering the economic aspects, the amount of 0.03 g of catalyst is selected as an optimum amount.

Finally, under the optimal conditions, benzaldehyde dimethyl acetals derivatives with various substitution groups and active methylene compounds (ethylcyanoacetate and malononitrile) were reacted (Table 6). It is seen that all the reactions are performed with high yields and relatively low reaction times. Furthermore, the reactions which were performed with the malononitrile as an active methylene compound show less reaction time and more yields than that of ethylcyanoacetate (Table 6, entries 19–25).

In the next step, Ni-Pd@poly (SSA-NVI)/KIT-6 nanocomposite was used as a promoter in the sequential one-pot deacetalization–Knoevenagel condensation-reduction reaction in water at 45 °C. In this reaction, the deacetalization step is performed by the acid groups of the catalyst, then Knoevenagel condensation is carried out by the basic groups of the catalyst, and finally, the metals catalyze the reduction step (Scheme 2).

The optimum conditions for this reaction were selected based on deacetalization–Knoevenagel condensation reaction and for the reduction step, sodium borohydride was selected as a reducing agent. The results for sequential one-pot deacetalization–Knoevenagel condensation-reduction reaction between different benzaldehyde dimethyl acetals and ethylcyanoacetate are presented in Table 7. According to the results, all the reactions were completed in considerable times and afforded the desired products in high yields. Moreover, looking the results, it can be found that in the reduction step, alkene and ester groups will reduce to alkane and alcohol, respectively, whilst, the nitrile group remained unreacted (Table 7, entries 1–8). It should be mentioned that even with increasing the amount of $NaBH_4$, it remained unreacted. It means that the catalyst can be used as a chemo-selective heterogeneous catalyst.

Also, the sequential one-pot three-step reaction of 3-nitro benzaldehyde dimethylacetal and ethylcyanoacetate was specifically studied (Table 7, entry 9). As can be seen, in the reduction step over Ni-Pd@poly (SSA-NVI)/KIT-6 catalyst, alkene (C=C), ester (CO_2Et) and nitro (NO_2)

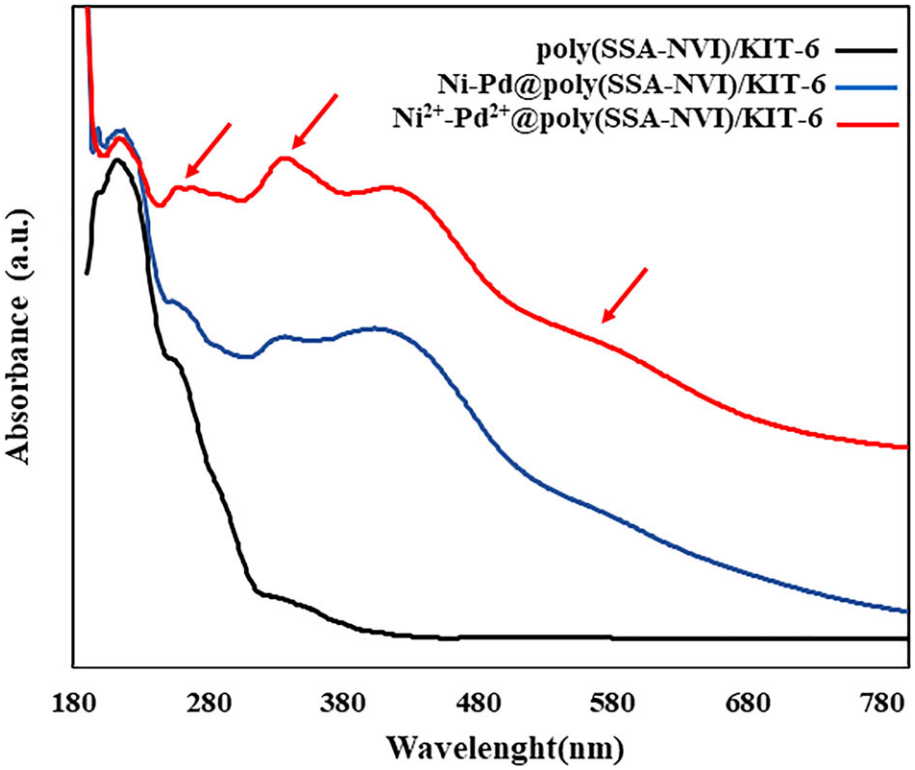

FIGURE 9 DRS UV–vis spectra of Ni-Pd@poly (SSA-NVI)/KIT-6, Ni^{2+}-Pd^{2+}@poly (SSA-NVI)/KIT-6 and poly (SSA-NVI)/KIT-6 samples

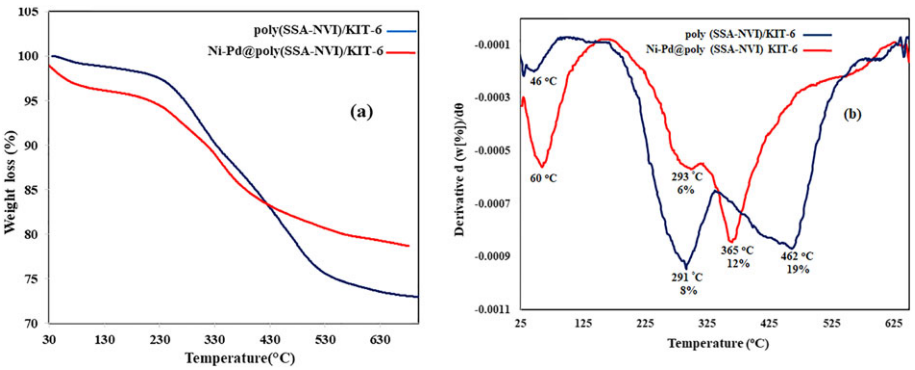

FIGURE 10 (a) TGA and (b) DTG curves of the poly (SSA-NVI)/KIT-6 and Ni-Pd@poly (SSA-NVI) KIT-6

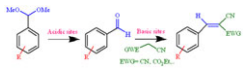

SCHEME 1 Sequential deacetalization-Knoevenagel condensation reaction

groups were completely reduced to alkane, alcohol, and amine in excellent yield (Scheme 3, product 2). However, nitrile group was still unreacted.

To achieve more useful results about the role of metals, the same reaction was repeated over Pd@poly (SSA-NVI)/KIT-6 and Ni@poly (SSA-NVI)/KIT-6 catalysts (Scheme 3). The results showed that the reaction which was performed over Pd@poly (SSA-NVI)/KIT-6 (Scheme 3, product 2) had the same results with Ni-Pd@-poly (SSA-NVI)/KIT-6. On the other hand, surprisingly, it was found that when nickel nanoparticle containing catalyst was used alone, the catalyst (Ni@poly (SSA-NVI)/KIT-6) even with high amounts of $NaBH_4$ was only able to reduce the ester and alkene groups (product 1) in a reasonable yield. These results were confirmed by the GC-Mass, ^{1}H NMR, ^{13}C NMR and FT-IR of the crude products. These results prove the chemo-selectivity of the catalysts prepared with different metals.

As we found that the metal nanoparticles show different catalytic activity and chemo-selectivity for the sequential one-pot deacetalization–Knoevenagel condensation-reduction reaction between 3-nitro

TABLE 2 Effect of monomer molar ratio and KIT-6 amount on catalytic activity of poly (SSA-NVI)/KIT-6 for one-pot deacetalization–Knoevenagel condensation reaction[a]

Entry	Monomer molar ratio (SSA:NVI)	Amount of KIT-6 (g)	Yield [%][b]
1	1:1	0.25	71
2	2:1	0.25	94
3	2:1	0.5	81
4	2:1	1	50
5	3:1	0.25	85

[a]Reaction condition: 3-nitro benzaldehyde dimethyl acetal (1 mmol), ethylcyanoacetate (1 mmol), catalyst (0.03 g) and H_2O (3 mL), 45 °C, reaction time: 30 min.

[b]Isolated yields.

benzaldehyde dimethyl acetal and ethylcyanoacetate, various catalysts with the different Ni:Pd molar ratios in 0.1 g poly (SSA-NVI)/KIT-6 were prepared and used in the desired reaction. In these reactions, the total amount of metals were fixed and considered 0.1 mmol. As we mentioned before, when only Ni nanoparticles have been immobilized into the catalyst, just ester and alkene groups were reduced and the nitro group remained unreacted while the catalytic performance was 76% in 90 min (Table S3). However, combining palladium with nickel nanoparticles shows the better catalytic activity and a different chemo-selectivity (ester, alkene and nitro groups were reduced). To evaluate this, different Ni:Pd molar ratios (0:100, 20:80, 30:70, 50:50, 70:30) have been tested and showed that the catalyst activities in all molar ratios were almost the same. However, due to the lower amount of Pd as an expensive metal used in the preparation of the catalyst, the catalyst prepared by Ni: Pd (70:30 molar ratio) was chosen as the best catalyst.

TABLE 5 Effect of amount of poly (SSA-NVI)/KIT-6 on sequential one-pot reaction of deacetalization–Knoevenagel condensation[a]

Entry	Amount of catalyst (g)	Yield [%][b]
1	0.01	86
2	0.03	94
3	0.05	95

[a]Reaction condition: 3-nitro benzaldehyde dimethyl acetal (1 mmol), ethylcyanoacetate (1 mmol) and H_2O (3 ml) at 45 °C, reaction time: 30 min.

[b]Isolated yields.

To the best of our knowledge, there are only two reports about the reduction of α-cyano-α,β-unsaturated esters.[39,40]

In one of them, Sudalai, et al reported the reduction of α-cyano-α,β-unsaturated esters using $NaBH_4$ over $CoCl_2$ as a homogeneous catalyst.[39] They performed the reaction in ethanol as solvent at 6 hr. For the reduction of ethyl-2-cyano-3-(3-nitrophenyl) acrylate, they achieved 2-(Hydroxymethyl)-3-(3-nitrophenyl) propanenitrile in 80% yield which means that they could reduce the alkane and esters to alkane and alcohols, respectively, but nitro and cyanide groups remained unreacted.

In other reports, Luis et.al reported two-step Knoevenagel reaction-reduction over a bifunctional catalyst containing Au nanoparticles.[40] They could reduce the alkane, ester and nitro groups to alkane, alcohol and amine groups at 24 hr using 20 mmol $NaBH_4$. Moreover, in all cases, the nitro group was reduced during the reaction.

TABLE 3 The amount of acid sites of the catalysts prepared by various monomer molar ratios

Entry	Monomer molar ratio (SSA:NVI)	Amount of polymer (g)	Theoretical amount of acid (mmol g^{-1})	Experimental amount of acid (mmol g^{-1})	Percentage[a] (%)
1	1:1	1	0.121	0.105	86
2	2:1	1	0.088	0.082	93
3	3:1	1	0.056	0.043	76

[a]The ratio of the experimental amount to the theoretical amount.

TABLE 4 The amount of base sites of the catalysts prepared by various monomer molar ratios

Entry	Monomer molar ratio (SSA:NVI)	Amount of polymer (g)	Theoretical value of base (mmol g^{-1})	Experimental value of base (mmol g^{-1})	Percentage[a] (%)
1	1:1	1	0.121	0.08	66
2	2:1	1	0.177	0.132	74
3	3:1	1	0.17	0.13	76

[a]The ratio of the experimental amount to the theoretical amount.

TABLE 6 Sequential one-pot deacetalization–Knoevenagel condensation reaction of different benzaldehyde dimethyl acetals and active methylene groups catalyzed by poly (SSA-NVI)/KIT-6[a]

Entry	Aryl carbaldehyde dimethyl acetal	Product	Time (h/min)	Yield[b] (%)
1	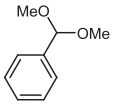	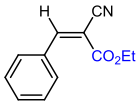	1.5	93
2	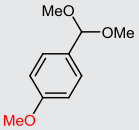	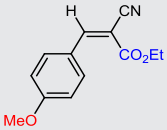	1.5	96
3	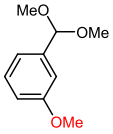	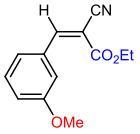	160 min	95
4	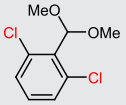	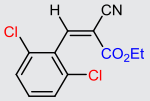	3.5	92
5	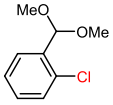	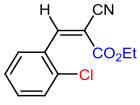	2	63
6	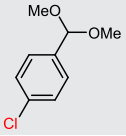	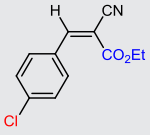	3	97
7	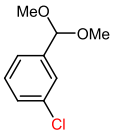	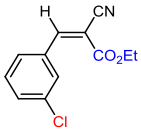	2	89
8	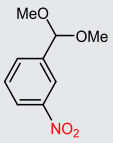	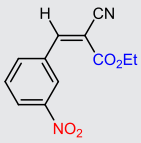	0.5	94
9	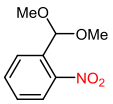	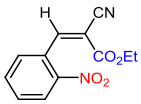	2	92
10	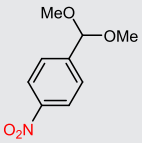	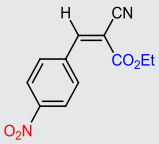	40 min	94
11	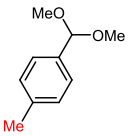	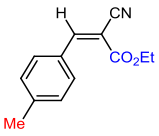	4.5	95
12	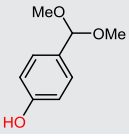	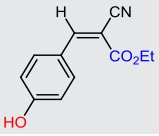	20 min	97
13	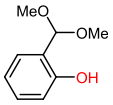	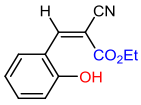	5	95

(Continues)

TABLE 6 (Continued)

Entry	Aryl carbaldehyde dimethyl acetal	Product	Time (h/min)	Yield[b] (%)
14	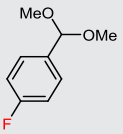	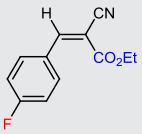	5	95
15	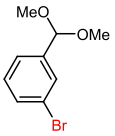	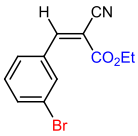	4	97
16	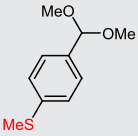	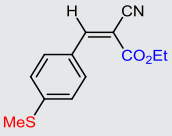	2.8	94
17	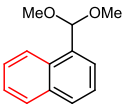	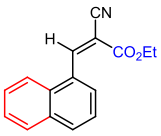	4.5	80
18	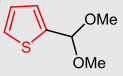	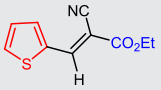	20	95
19	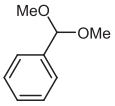	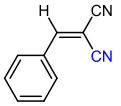	1	95
20	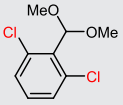	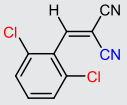	70 min	94
21	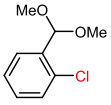	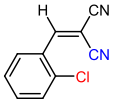	0.5	92
22	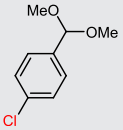	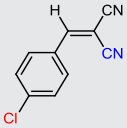	0.5	85
23	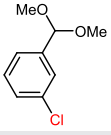	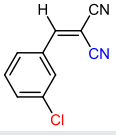	40 min	96
24	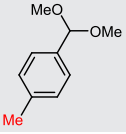	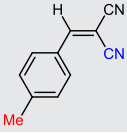	**50 min**	90
25	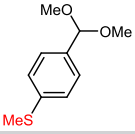	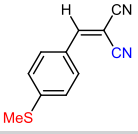	20 min	95

[a]Reaction condition: Aryl carbaldehyde dimethyl acetal (1 mmol), active methylene compound (1 mmol), catalyst (0.03 g) and H_2O (3 ml) at 45 °C.

[b]Isolated yields.

SCHEME 2 Sequential one-pot deacetalization–Knoevenagel condensation-reduction reaction

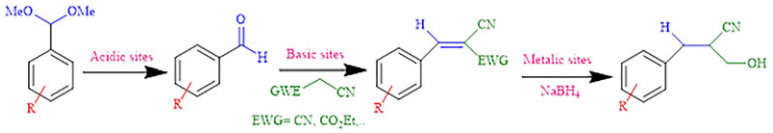

TABLE 7 Sequential one-pot deacetalization–Knoevenagel condensation-reduction reaction of different benzaldehyde dimethyl acetal catalyzed by Ni-Pd@poly (SSA-NVI)/KIT-6[a]

Entry	Benzaldehyde dimethyl acetal	Product	Total time (h/min)	Reduction Time (h/min)	Yield[b] (%)
1	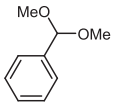	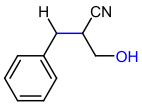	2.5	1	90
2	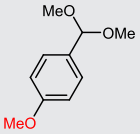	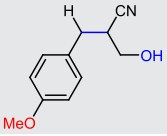	2.5	1	94
3	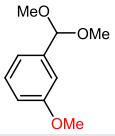	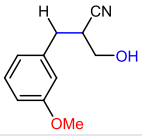	220 min	1	93
4	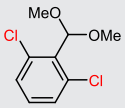	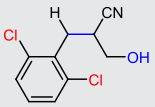	5.5	2	87
5	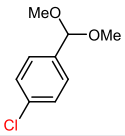	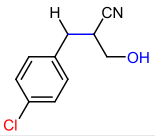	220 min	40 min	95
6	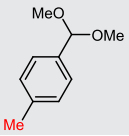	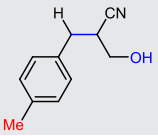	310 min	40 min	90
7	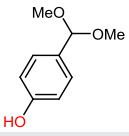	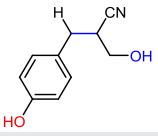	1	40 min	95
8	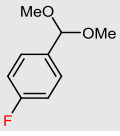	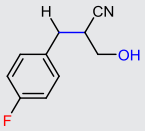	325 min	25 min	93
9	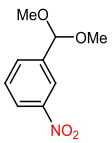	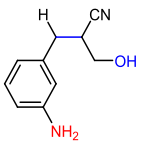	50 min	20 min	94[c]

[a]Reaction condition: Aryl carbaldehyde dimethyl acetal (1 mmol), ethylcyanoacetate (1 mmol), catalyst (0.03 g), Ni:Pd molar ratio (70:30), $NaBH_4$ (2 mmol), H_2O (3 mL), 45 °C.

[b]Isolated yields.

[c]$NaBH_4$ (6 mmol).

In compare, our catalyst could act as a heterogeneous tri-functional catalyst to catalyze the sequential one-pot deacetalization–Knoevenagel condensation-reduction in water as a green solvent and the reaction was done at just 50 min. Moreover, it could be used for the reduction of alkene, ester and nitro groups or alkene and ester by a

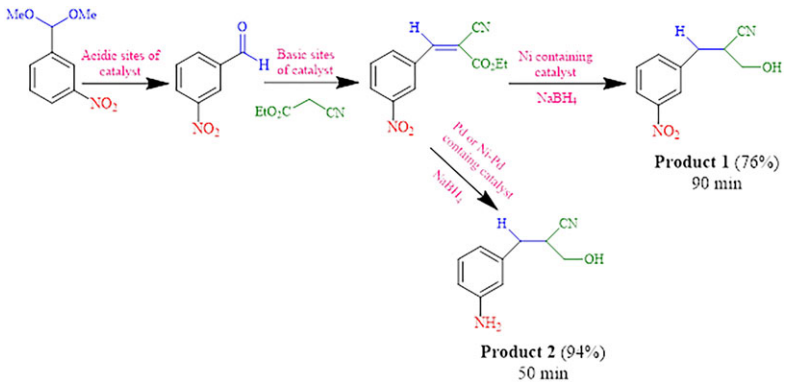

SCHEME 3 Sequential one-pot deacetalization–Knoevenagel condensation-reduction reaction between 3-nitro benzaldehyde dimethyl acetal and ethylcyanoacetate over different metal-containing catalysts

simple change in the structure of the catalyst. In addition, it could be reused for several times.

To ensure the heterogeneity nature of the catalyst, the one-pot sequential reaction between 3-nitro benzaldehyde dimethyl acetal and ethylcyanoacetate was started. Then, it was stopped after 40 min and the catalyst was separated from the reaction mixture by filtration. Then, the reaction was continued for an extra 5 hr without the catalyst. The results showed that the reaction was not progressed after filtering the catalyst, means that the reaction was carried out on the heterogeneous surface of Ni-Pd@poly (SSA-NVI)/KIT-6. It should be mentioned that according to the results of HPLC analysis, polymer leaching was not seen during the reaction.

Also, the reusability of Ni-Pd@poly (SSA-NVI)/KIT-6 catalyst was studied in the above-mentioned reaction. In this way, the catalyst was separated by filtering after the completion of the reaction, then washed with diethyl ether, acetone, and water (or ethanol and water), and dried at 60 °C for 3 hr. Then the recovered catalyst immediately reused in the same fresh reaction without any pre-activation. The results depicted that the synthesized catalyst could be reused 7 times with acceptable catalytic activity (Figure S17).

The FE-SEM images of recycled catalyst exhibited that the structure of the fresh catalyst is maintained even after the sixth run (Figure 11). Also, EDS analysis and FE-SEM-mapping of the reused catalyst after the sixth

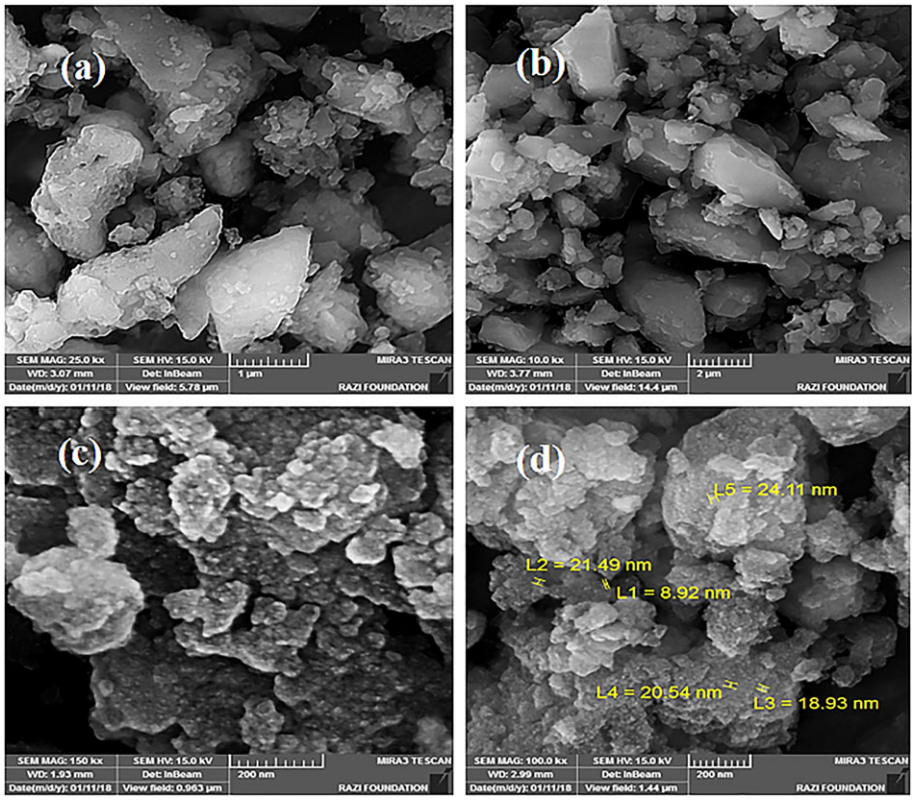

FIGURE 11 FESEM image of the reused catalyst after the sixth run

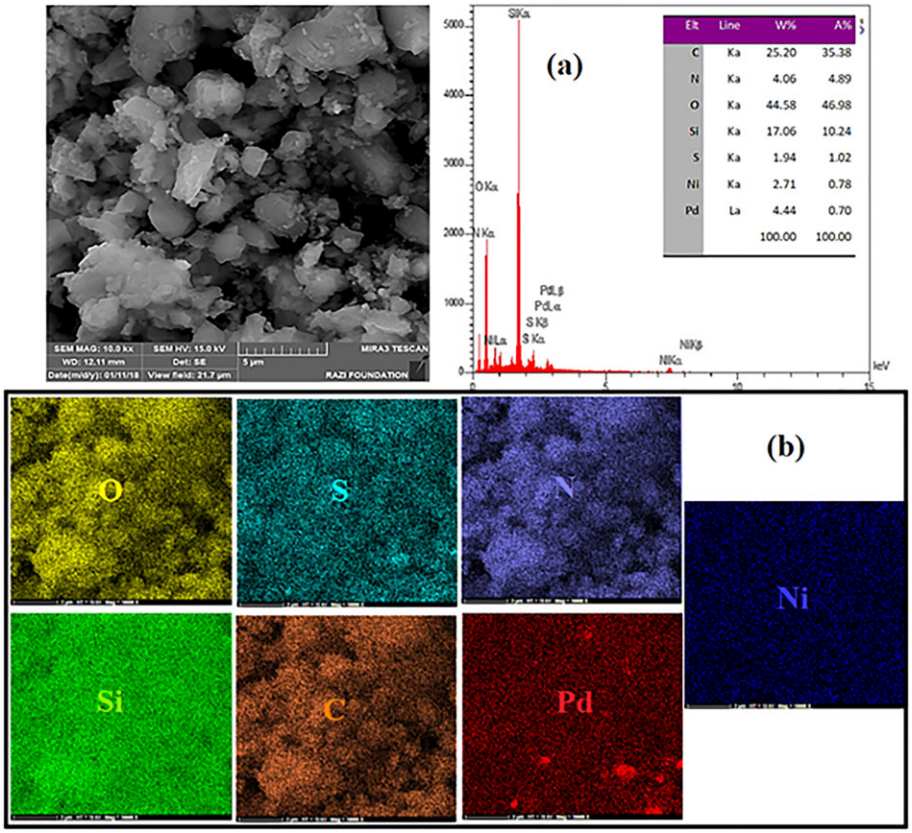

FIGURE 12 (a) EDS analysis and (b) FESEM-elemental-mapping images of reused catalyst after the sixth run

run showed the suitable distribution of Pd and Ni nanoparticles on the surface (Figure 12).

Moreover, the low-angle XRD pattern of the recovered catalyst after the sixth run displayed the same pattern of fresh catalyst (Figure S18a). Also, the wide-angle XRD pattern of the reused catalyst showed the presence of Pd NPs on the surface of the catalyst after the sixth run (Figure S18b).

Furthermore, ICP-AES results show 0.0211 mmol g^{-1} Pd and 0.0470 mmol g^{-1} Ni content of recycled catalyst after the sixth run that represented only 0.9% and 1.2% leaching for Pd and Ni, respectively. Therefore, the decrease in catalyst activity after the sixth run is probably due to low leaching of Ni-Pd or aggregations of nanoparticles on the surface of the support.

4 | CONCLUSIONS

We have demonstrated a novel acid–base-metal trifunctional catalyst comprising Ni-Pd@poly (SSA-NVI)/KIT-6 using simple and facile methods. To prepare this catalyst, firstly, we synthesized bifunctional heterogeneous crosslinked polymer as an acid–base function of catalyst in the pores of KIT-6, for the first time. We used thiol-ene click reaction through the free-radical chain transfer mechanism with special features including 1. High efficiency; 2. Uniform distribution of monomers in the polymer network; 3. Water and oxygen insensitivity; 4. Minimal side products; 5. High reaction rates. Also, another feature of this polymerization reaction is minimizing the acid and base neutralization due to the presence of cross-linkers and sufficient space between them.

After preparation and characterization of Ni-Pd@poly (SSA-NVI)/KIT-6, we used this catalytic system to catalyze the three-step one-pot deacetalization-Knoevenagel condensation-reduction reaction. In the reduction step, this catalyst was able to reduce the C=C bond, ester (CO_2Et) and nitro (NO_2) groups in high yield. The important point is that the catalyst was able to make catalytic chemo-selectivity by changing the metal combination from alone Ni to Ni-Pd mixture (alloy) and reduced the nitro (NO_2) group in addition to the C=C, ester (CO_2Et) groups while nitrile group remains unchanged.

ACKNOWLEDGEMENTS

The authors would like to acknowledge financial support from Kharazmi University.

ORCID

Roozbeh Javad Kalbasi https://orcid.org/0000-0003-3975-6609

REFERENCES

[1] C. You, C. Yu, X. Yang, Y. Li, H. Huo, Z. Wang, Y. Jiang, X. Xu, K. Lin, *New J. Chem.* **2018**, *42*, 4095.

[2] S. Sobhani, F. Zarifi, J. Skibsted, *New J. Chem.* **2017**, *41*, 6219.

[3] H. Liu, F. G. Xi, W. Sun, N. N. Yang, E. Q. Gao, *Inorg. Chem.* **2016**, *55*, 5753.

[4] M. J. Climent, A. Corma, S. Iborra, *Chem. Rev.* **2010**, *111*, 1072.

[5] Z. Jia, K. Wang, B. Tan, Y. Gu, *ACS Catal.* **2017**, *7*, 3693.

[6] D. Wang, B. Wang, Y. Ding, H. Wu, P. Wu, *Chem. Commun.* **2016**, *52*, 12817.

[7] T. Toyao, M. Fujiwaki, Y. Horiuchi, M. Matsuoka, *RSC Adv.* **2013**, *3*, 21582.

[8] P. Li, C. Y. Cao, H. Liu, Y. Yu, W. G. Song, *J. Mater. Chem. A* **2013**, *1*, 12804.

[9] F. Zhang, H. Jiang, X. Li, X. Wu, H. Li, *ACS Catal.* **2013**, *4*, 394.

[10] L. C. Lee, J. Lu, M. Weck, C. W. Jones, *ACS Catal.* **2016**, *6*, 784.

[11] L. Xiong, H. Zhang, Z. He, T. Wang, Y. Xu, M. Zhou, K. Huang, *New J. Chem.* **2018**, *42*, 1368.

[12] P. Li, Y. Yu, H. Liu, C. Y. Cao, W. G. Song, *RSC Nanoscale* **2014**, *6*, 442.

[13] A. V. Biradar, V. S. Patil, P. Chandra, D. S. Doke, T. Asefa, *Chem. Commun.* **2015**, *51*, 8496.

[14] K. Nakabayashi, H. Mori, *Eur. Polym. J.* **2013**, *49*, 2808.

[15] C. E. Hoyle, C. N. Bowman, *Angew. Chem. Int. Ed.* **2010**, *49*, 1540.

[16] C. E. Hoyle, A. B. Lowe, C. N. Bowman, *Chem. Soc. Rev.* **2010**, *39*, 1355.

[17] R. Gharibi, H. Yeganeh, Z. Abdali, *J. Mater. Sci.* **2018**, *53*, 1581.

[18] C. Peng, W. Pan, L. Bao, S. Chen, Y. Chen, M. Han, Y. Xiong, W. Xu, *Polym. Adv. Technol.* **2014**, *25*, 684.

[19] B. J. Sparks, T. J. Kuchera, M. J. Jungman, A. D. Richardson, D. A. Savin, S. Hait, J. Lichtenhan, M. F. Striegel, D. L. Patton, *J. Mater. Chem.* **2012**, *22*, 3817.

[20] S. Hafeez, L. Barner, L. Nebhani, *Macromol. Rapid Commun.* **2018**, *39*, 1800169.

[21] M. Zhu, B. He, W. Shi, Y. Feng, J. Ding, J. Li, F. Zeng, *Fuel* **2010**, *89*, 2299.

[22] C. Fodor, J. Bozi, M. Blazso, B. Ivan, *Macromolecules* **2012**, *45*, 8953.

[23] W. Dai, M. Zheng, Y. Zhao, S. Liao, G. Ji, J. Cao, *Nanoscale Res. Lett.* **2009**, *5*, 103.

[24] Y. Teng, X. Wu, Q. Zhou, C. Chena, H. Zhao, M. Lan, *Sens Actuators B Chem.* **2009**, *142*, 267.

[25] P. Wang, Z. Wang, J. Li, Y. Bai, *Microporous Mesoporous Mater.* **2008**, *116*, 400.

[26] M. S. Ahmed, S. Jeon, *ACS Catal.* **2014**, *4*, 1830.

[27] C. Tang, Y. Liu, C. Xu, J. Zhu, X. Wei, L. Zhou, L. He, W. Yang, L. Mai, *Adv. Funct. Mater.* **2017**, *28*, 1704561.

[28] T. W. Kim, F. Kleitz, B. Paul, R. Ryoo, *J. Am. Chem. Soc.* **2005**, *127*, 7601.

[29] M. Rezaei, A. N. Chermahini, H. A. Dabbagh, *Chem. Eng. J.* **2017**, *314*, 515.

[30] L. Xu, C. Wang, J. Guan, *J. Solid State Chem.* **2014**, *213*, 250.

[31] R. Kishor, A. K. Ghoshal, *RSC Adv.* **2016**, *6*, 898.

[32] Y. Teng, X. Wu, Q. Zhou, C. Chen, H. Zhao, M. Lan, *Sens Actuators B Chem.* **2009**, *142*, 267.

[33] R. Kishor, A. K. Ghoshal, *Chem. Eng. J.* **2015**, *262*, 882.

[34] H. Wu, A. Duan, Z. Zhao, T. Li, R. Prins, X. Zhou, *J. Catal.* **2014**, *317*, 303.

[35] M. Li, B. Li, H. F. Xia, D. Ye, J. Wu, Y. Shi, *Green Chem.* **2014**, *16*, 2680.

[36] X. Zhang, P. Zhang, H. Yu, Z. Ma, S. Zhou, *Catal Letters.* **2015**, *145*, 784.

[37] D. Tessier, A. Rakai, F. Bozon-Verduraz, *J. Chem. Soc., Faraday Trans.* **1992**, *88*, 741.

[38] G. Vijayakumar, A. Pandurangan, *Energy* **2017**, *140*, 1158.

[39] A. R. Jagdale, A. S. Paraskar, A. Sudalai, *Synthesis* **2009**, *4*, 660.

[40] S. Montolio, C. Vicent, V. Aseyev, I. Alfonso, M. I. Burguete, H. Tenhu, E. García-Verdugo, S. V. Luis, *ACS Catal.* **2016**, *6*, 7230.

SUPPORTING INFORMATION

Additional supporting information may be found online in the Supporting Information section at the end of the article.

How to cite this article: Javad Kalbasi R, Mesgarsaravi N, Gharibi R. Synthesis of multifunctional polymer containing Ni-Pd NPs via thiol-ene reaction for one-pot cascade reactions. *Appl Organometal Chem*. 2019;e4800. https://doi.org/10.1002/aoc.4800